Journal of Molecular Structure 1083 (2015) 88–94

Contents lists available at ScienceDirect

Journal of Molecular Structure

journal homepage: www.elsevier.com/locate/molstruc

A supramolecular structure based on copper complex of 2,3-pyridinedicarboxylic acid and 1,3-bis(3-aminopropyl) tetramethyldisiloxane chlorohydrate

Alina Soroceanu, Alexandra Bargan, Sergiu Shova, Mihaela Avadanei, Maria Cazacu *

"Petru Poni" Institute of Macromolecular Chemistry, Aleea Gr. Ghica Voda 41A, 700487 Iasi, Romania

HIGHLIGHTS

- 3D supramolecular architecture built up on the basis of two complex entities was obtained.
- X-ray crystallography revealed the obtained crystalline compound to have an ionic structure.
- Complex structure preserves at heating in solid state and recovers from solution after solvent removal.
- Theoretical estimation revealed the sorption suitability for small molecules only.

GRAPHICAL ABSTRACT

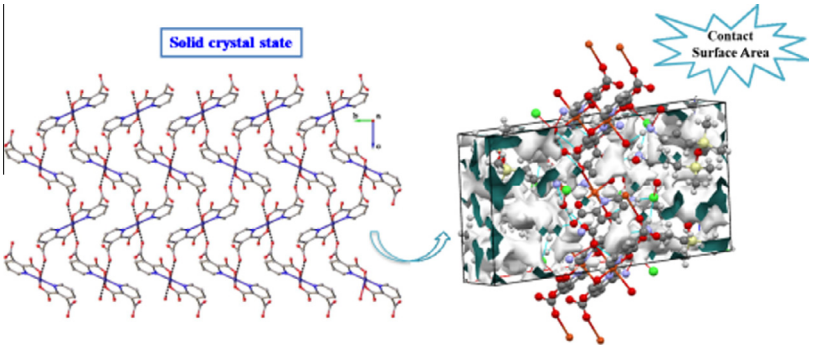

ARTICLE INFO

Article history:
Received 8 August 2014
Received in revised form 2 November 2014
Accepted 17 November 2014
Available online 21 November 2014

Keywords:
Copper complex
Supramolecular structure
Structural analysis
Thermal stability
Siloxane diamine
2,3-Pyridinedicarboxylic acid

ABSTRACT

Having in mind the synthesis of a cooper complex with the product of condensation between an anhydride and a siloxane diamine as a new polydentate ligand, 2,3-pyridinedicarboxylic anhydride (PDCA) was treated first with 1,3-bis(3-aminopropyl)tetramethyldisiloxane (AP_0) and then with cooper chloride in alcoholic solution. However, according to single-crystal X-ray crystallography and IR spectroscopy, the reaction resulted in an ionic compound with the charge balance in agreement with the formation of **$[H_2AP_0]_2[Cu(PDC)_2]\cdot Cl_2\cdot 2H_2O$** species, where PDC is a double deprotonated 2,3-pyridinedicarboxylic acid. The thermal and moisture behaviors of the complex were studied by thermogravimetrical analysis and dynamic vapor sorption, respectively. The stability of the supramolecular structure with temperature and in methanol solution was studied by ATR-FTIR analysis.

Introduction

The coordination compounds built on transition metal and multicarboxylate ligands are intensely studied due to their large potential applications. They can form extended supramolecular structures with various architectures and topologies by self-assembling of metal–organic units via hydrogen bonds and π–π interactions. The key in the designing of the desired structure is the proper selection of the metal ion and ligand. Polycarboxylic ligands are good candidates because they can function both as proton donor and as acceptor in the hydrogen bond depending on the number of the deprotonated carboxylic groups [1]. Pyridine dicarboxylic acids have proved to be interesting and important ligand because they exhibit various coordination modes [2–7]. Due to the manifold N- and O-donors of pyridine dicarboxylic ligands, these can form

* Corresponding author.
E-mail address: mcazacu@icmpp.ro (M. Cazacu).

http://dx.doi.org/10.1016/j.molstruc.2014.11.038
0022-2860/

with metals versatile structural motifs, which finally aggregate to generate various supramolecular architectures with interesting properties [8]. As one of the dicarboxylate ligands, 2,3-pyridinedicarboxylic acid has drawn extensive attention [8–10]. This acid often acts as a bidentate chelating ligand through the nitrogen atom and one oxygen atom of the carboxylic group to form a discrete complex [11] and 2-D layer [12].

In this paper, our intention was to react 2,3-pyridinedicarboxylic anhydride with a siloxane diamine, 1,3-bis(3-aminopropyl)tetramethyldisiloxane, and to complex the product with a copper salt, $CuCl_2$. Similar reactions between dicarboxylic acids and amine in general lead to amic acids or mixture of these with cyclic imides [13]. Due to its high reactive groups, 1,3-bis(3-aminopropyl)tetramethyldisiloxane is an important silicone derivative useful for the incorporation of the siloxane sequences in a large range of the siloxane–organic copolymers having amide [14,15], imide [16–18], or imine [19–25] internal functional groups. The last functional group mainly is very useful for the metal complexation. The presence of the highly flexible tetramethyldisiloxane moiety might confer them higher conformational flexibility useful in catalysis [26] and besides its high hydrophobicity also to increase the solubility in common organic solvents and lower the thermal transitions of the complexes thus improving their processability. The biocompatibility and physiological inertness of the siloxane is an advantage in future use of the resulted derivatives in biomedical field. The reaction product separated as a crystalline phase was characterized by spectral (FTIR and UV–Vis) methods and single crystal X-ray diffraction. The stability of the supramolecular structure with temperature as well as in methanol was studied by FTIR while the capacity of gas storage was theoretical estimated on the basis of crystallographic data.

Experimental

Materials

2,3-pyridinedicarboxylic anhydride, PDCA, (purum, ⩾98%, m.p. 136–139 °C), copper(II) chloride dihydrate, $CuCl_2{\cdot}2H_2O$ (ACS reagent, ⩾99%, m.p. 100 °C) and N,N-dimethylformamide, DMF (⩾99.8, b.p. 153 °C, density 0.944 g/mL) were purchased from Sigma-Aldrich, while 1,3-bis(3-aminopropyl)tetramethyldisiloxane, $[H_2N(CH_2)_3(CH_3)_2Si]_2O$, AP_0 (b.p. = 142 °C/11.5 mmHg, d^4_{20} = 0.901), was acquired from Fluka AG. Solvents: methanol p.a. (d^{20} = 0.792 g/mL), chloroform p.a. (d^{20} = 1.48 g/mL), were received from Chemical Company (Romania).

Measurements

Given the purpose of the paper, the following techniques were used:

FTIR spectroscopy was chosen for a primary structural characterization; because the compound was isolated as a single crystal, the structure presumed on the basis of IR spectrum could be confirmed by single-crystal X-ray diffraction. Due to the presence of supramolecular bonds emphasized by above techniques, it was of interest to study the thermal stability of the structure by using thermogravimetric analysis and ATR-FTIR spectroscopy, stability in solution (in a polar solvent, e.g., methanol) also monitored by ATR-FTIR spectroscopy, and behavior against moisture studied by water vapor sorption in dynamic mode.

Infrared spectra were recorded using a Bruker Vertex 70 FTIR spectrometer having integrated OPUS operation and evalution software, in the transmission mode (KBr pellets) between 4000 and 400 cm^{-1} at room temperature with a resolution of 2 cm^{-1} and accumulation of 32 scans. Attenuated total reflectance-Fourier transform infrared (ATR-FTIR) spectra were recorded using a Bruker Vertex 70 FTIR spectrometer equipped with a zinc selenide (ZnSe) ATR crystal. Registrations were performed on liquid samples (0.020 g complex in 1 mL methanol) in ATR mode in the 600–4000 cm^{-1} in the room temperature −140 °C range at with a resolution of 4 cm^{-1} and accumulation of 32 scans.

The thermogravimetric (TG) – differential thermogravimetric (DTG) analysis was performed on a STA 449 F1 Jupiter NETZSCH equipment running under Proteus Software. The measurements were made in the temperature 20–700 °C range under a nitrogen flow (50 mL min^{-1}) using a heating rate of 10 °C min^{-1}. Alumina crucible was used as sample holder.

Water vapor sorption (DVS) capacity of the sample has been determined in dynamic regime in the relative humidity (RH) range 0–90% by using the fully automated gravimetric analyzer IGAsorp produced by Hiden Analytical, Warrington (UK). The sample was placed in a special container and dried at 25 °C in flowing nitrogen (250 mL/min) until it reaches a constant weight at RH < 1%. Then, the relative humidity (RH) was gradually increased from 0 to 90%, in 10% humidity steps, each step having a pre-established equilibrium time between 10 and 20 min so as the sorption equilibrium to be achieved every time. When RH decreased, desorption curves were recorded.

X-ray crystallography

Crystallographic measurements were carried out with an Oxford-Diffraction XCALIBUR E CCD diffractometer equipped with graphite-monochromated Mo Kα radiation. Single crystals were positioned at 40 mm from the detector and 186 frames were measured each for 10 s over 1° scan. The unit cell determination and data integration were carried out using the CrysAlis package of Oxford Diffraction [27]. The structure was solved by direct methods using Olex2 [28] software with the SHELXS structure solution program and refined by full-matrix least-squares on F^2 with SHELXL-97 [29]. Atomic displacements for non-hydrogen atoms were refined using an anisotropic model. All H atoms attached to carbon were introduced in idealized positions (d_{C-H} = 0.96 Å) using the riding model with their isotropic displacement parameters fixed at 120% of the riding atom. The positional parameters of OH and NH hydrogen atoms were found from difference Fourier syntheses and verified by the geometric parameters of the corresponding hydrogen bonds. The molecular plots were obtained using the Olex2 program. Table 1 provides a summary of the crystallographic data together with refinement details for compounds **1**. CCDC 1002444 contains the supplementary crystallographic data for this contribution. These data can be obtained free of charge from the Cambridge Crystallographic Data Centre via www.ccdc.cam.ac.uk/data_request/cif.

Procedure

In a round bottom flask were loaded 1.073 g (7.2 mmol) of PDCA, 1 mL (0.897 g, 3.6 mmol) AP_0 and 10 mL of DMF. The mixture was stirred at room temperature for 1 h and then heated for 5 h at 140 °C after which left in rest at room temperature. The next day, the reaction mixture was distilled in vacuum to remove the solvent and other volatile fraction, eventually. The rest solid was dissolved in 12 mL methanol and then a solution consisting in 0.613 g (3.6 mmol) copper chloride and 6 mL methanol was added over it. The new resulting mixture was stirred for 5 min at room temperature and then was allowed to crystallize. Formation of blue prismatic crystals was observed after about two years. These were separated by filtration washed with methanol, dried in air and further analyzed (compound **1**), the rest being a complex mixture, amorphous, difficult to separate. Yield 1.153 g (32%).

Table 1
Crystallographic data, details of data collection and structure refinement parameters for **1**.

Empirical formula	$C_{34}H_{70}CuCl_2N_6O_{12}Si_4$
Formula weight	1001.76
Temperature/K	200
Crystal system	Monoclinic
Space group	$P2_1/c$
a/Å	23.527(3)
b/Å	7.9089(7)
c/Å	13.6772(13)
α/°	90
β/°	94.627(10)
γ/°	90
V/Å^3	2536.7(4)
Z	2
D_{calc}/mg/mm^3	1.312
μ/mm^{-1}	0.687
Crystal size/mm^3	0.40 × 0.20 × 0.03
θ_{min}, θ_{max} (°)	3.48–49.42
Reflections collected	7349
Independent reflections	4287[R_{int} = 0.0461]
Data/restraints/parameters	4287/0/277
R_1[a]($I > 2\sigma(I)$)	0.0778
wR_2[b](all data)	0.1712
GOF[c]	1.088
Largest diff. peak/hole/e Å^{-3}	0.71/−0.47

[a] $R_1 = \sum||F_o| - |F_c||/\sum|F_o|$.
[b] $wR_2 = \{\sum[w(F_o^2 - F_c^2)^2]/\sum[w(F_o^2)^2]\}^{1/2}$.
[c] GOF = $\{\sum[w(F_o^2 - F_c^2)^2]/(n-p)\}^{1/2}$, where n is the number of reflections and p is the total number of parameters refined.

$C_{34}H_{70}CuCl_2N_6O_{12}Si_4$ (1001.76 g/mol): %, calcd.: C 40.73, H 7.00, N 8.38; found: C 40.34, H 6.82, N 8.39. IR (KBr pellet, selected bands): 3391m, 3040m, 2956, 2554vw, 2453vw, 2104w, 1658s, 1637s, 1570s, 1504m, 1470m, 1440m, 1391s, 1361vs, 1272m, 1256s, 1236m, 1169w, 1138s, 1054s, 1001m, 955m, 875m, 842s, 835s, 828s, 7987s, 788s, 765m, 722m, 712m, 703m, 693m, 635w, 608w, 558vw, 483m, 440w. UV–Vis (DMF): λ_{max} (ε) = 374 nm (19534.18 L mol^{-1} cm^{-1}).

Results and discussion

The work idea was to prepare the amic acid derived from 2,3-pyridine dicarboxylic anhydride and a siloxane diamine, 1,3-bis(3-aminopropyl)tetramethyldisiloxane, and to use it as a dicarboxylate ligand for the complexation of the metal, i.e. copper. For this, the two organic components were heated together in a first phase and only further treated with metal salt at room temperature. A crystalline fraction, **1**, was formed after long time in this mixture which was isolated by filtration cleaned with methanol and dried and only this was taken into the further study. The presence of water traces was probable reason for the formation of carboxylic acid derivative.

In FTIR spectrum (Fig. 1S) of the crystalline compound, the bands characteristic for free and H-bond groups at 3391 and 3040 cm^{-1}, asymmetric C=O stretch from carboxylate group at 1658 cm^{-1} and for C=N from pyridine ring at 1570 cm^{-1} are visible. The presence of the dimethylsiloxane units is proved mainly by the absorption bands at 1256 cm^{-1} (Si—CH_3) and 1054 cm^{-1} (Si—O—Si).

The result of single-crystal X-ray diffraction study of compound **1** is shown in Fig. 1 and the interatomic distances and angles are summarized in Table 1S. X-ray crystallography revealed the crystal **1** to have an ionic structure built up from $\mathbf{[H_2AP_0]^{2+}}$ cations, $\mathbf{[Cu(PDC)_2]^{2-}}$ and $\mathbf{Cl^-}$ anions and solvate water molecules with the charge balance in agreement with the formation of species $\mathbf{[H_2AP_0]_2[Cu(PDC)_2]\cdot Cl_2\cdot 2H_2O}$. There are a quite strong intermolecular interactions between all the components of the

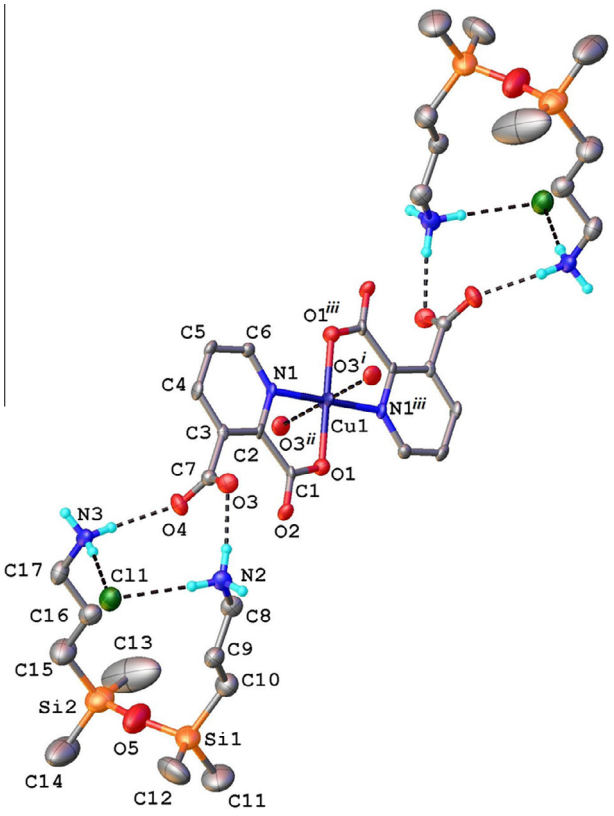

Fig. 1. X-ray structure of the $\mathbf{[H_2AP_0]_2[Cu(PDC)_2]\cdot Cl_2\cdot 2H_2O}$ unit in the crystal structure **1** with thermal ellipsoids at 50% probability level. Non-relevant H-atoms are omitted.

structure supported by N—H···O and N—H···Cl hydrogen bonding (see Table 2). The coordination geometry of cooper atom in $\mathbf{[Cu(PDC)_2]^{2-}}$ is a strongly distorted octahedron and the complex anion displays crystallographic inversion symmetry. The equatorial sites of the Cu^{II} atom are occupied by two double-deprotonated 2,3-pyridinedicarboxylate ligands as N,O-chelating ligands (Fig. 1).

The carboxylic group in the pyridine 3 position is almost perpendicular to pyridine ring with the dihedral angle between two planes of 92.8°. At the same time the carboxylic group in the pyridine 2 position is coplanar with pyridine ring within 0.11 Å. The axial positions are coordinated two O3^i and O3^{ii} atoms of the carboxylic groups of adjacent complex cations at the pyridine 3 positions at considerably longer Cu1—O3^i ($1-x$, $-y$, $-z$) and Cu1—O3^{ii} (x, $1/2-y$, $-1/2+z$) 2.787(3) Å distances giving rise to a Jahn-Teller distortion around the Cu^{2+} ion. It is important to note that, due to these weak Cu1—O3 interactions, the anionic $\mathbf{[Cu(PDC)_2]^{2-}}$ entities are linked to form a coordination polymer in two-dimensional architecture with Cu1···Cu1^i separation of 7.900(4) Å, as shown in Fig. 2.

In the crystal space packing, the arrangement of these two-dimensional layers parallel to 1 1 0 plane are alternately separated by the double layers formed by non-coordinated $\mathbf{[H_2AP_0]^{2+}}$ cations and water molecules. The $\mathbf{[H_2AP_0]^{2+}}$ units adopt a fully *cis*-oide conformation and act as pillars between separated $\mathbf{\{[Cu(PDC)_2]^{2-}\}_n}$. The interactions between two alternating layers occur through the intermolecular N—H···O, N—H···Cl, O—H···Cl and O—H···O H-bonding H-bonded, where the oxygen atom of the coordinated PDC^{2-} ligands act as acceptors. The view of packing diagram is shown in Fig. 3.

Thermogravimetry was used to evaluate the thermal stability of compound **1**. The analysis was performed in an inert atmosphere to prevent oxidation or other undesired reactions. The first stage

Table 2
H-bonds parameters.

D—H···*A*	*D*—H, Å	H···*A*, Å	*D*···*A*, Å	*D*—H···*A*, °	Symmetry code
N2—H···O3	0.89	1.89	2.768(5)	171.2	*x*, *y*, *z*
N2—H···O1*w*	0.89	2.00	2.818(6)	150.6	+*x*, 1/2 − *y*, 1/2 + *z*
N2—H···Cl1	0.89	2.35	3.243(5)	176.3	*x*, *y*, *z*
N3—H···O4	0.89	1.99	2.821(5)	154.3	*x*, *y*, *z*
N3—H···Cl1	0.89	2.24	3.117(5)	169.8	*x*, *y*, *z*
N3—H···O2	0.89	1.91	2.778(5)	164.5	+*x*, 1 + *y*,+*z*
O1*w*—H···O4	0.8	2.09	2.922(5)	167.6	*x*, *y*, *z*
O1*w*—H···Cl1	0.85	2.34	3.139(4)	157.7	+*x*, 3/2 − *y*, −1/2 + *z*

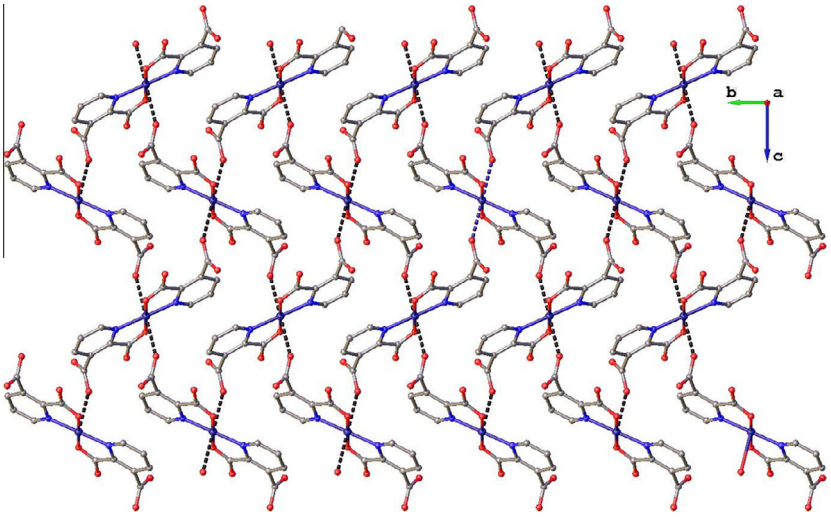

Fig. 2. 2D coordination network in crystal structure **1**.

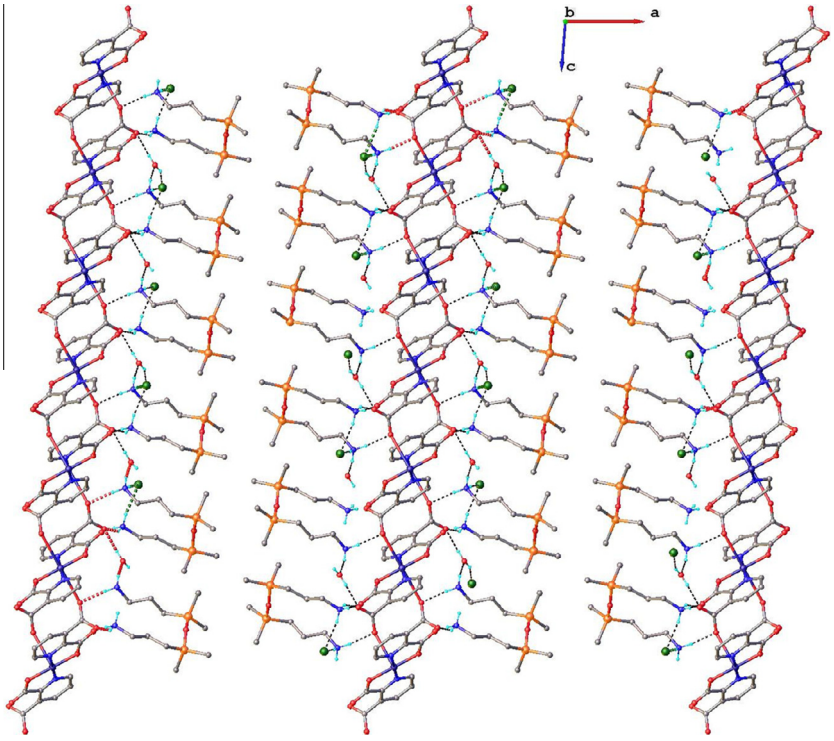

Fig. 3. The packing diagram along *b* crystallographic axis.

Table 3
The main parameter of the thermogravimetric curve.

Step	T (°C)			Mass change (%)
	T_{on}[a]	T_{max}[b]	T_{off}[c]	
I	146.74	159.89 176.36	184.56	5.50
II	215.81	236.20	262.66	34.28
III	313.03	350.09	376.68	31.96
IV	558.34	562.86	558.34	0.31

[a] The temperature at which the thermal degradation begins.
[b] The temperature at which the degradation rate reaches its maximum value.
[c] The temperature at which the process ends.

of the thermal decomposition starts at 146.7 °C and ends at 184.56 °C (maximum decomposition peak 159.89 °C) with a mass loss of 5.50% (Fig. 2S and Table 3). This first event is mainly assigned to the loss of the solvate water molecules that represent 3.60% from the mass of the compound and some solvent traces, probably. In the next two consecutive steps that begin at 215.81 with maxima at 236.2 and 350.09 and ending at 569.3, evaporation of 1,3-bis(3-aminopropyl)tetramethyldisiloxane followed by the decomposition of the carboxylate ligand occur. The final decomposition residue of 27.35 wt% probably consists in silica and copper oxides (theoretical value: 26.2%).

In order to study the behavior of the supramolecular crystalline compound in the presence of the humidity, the sorption-desorption isotherms were registered in dynamic regime, at three different temperatures, 25, 55, and 70 °C, by modifying (increasing and decreasing, respectively) the relative humidity in steps of 10%, with pre-established equilibrium times between 10 and 20 min (Fig. 3S and Table 2S). The isotherm recorded at room temperature could be associated with an isotherm of type III, according to IUPAC classification describing weak adsorbate-adsorbent interactions. The presence in crystal structure of the tetramethyldisiloxane units well-known for their hydrophobic character contributes to this behavior. The maximum sorption capacity value was 3.93 wt% at 25 °C. Desorption process occurs more slowly that sorption and about 0.5 wt% water is retained in sample. At higher temperatures (55 and 70 °C), the shape of the isotherms changes by the fact that due to the heating, the desorption rate approaches the sorption one reducing the hysteresis loop. The maximum sorption capacity increases to 7.29 at 55 °C but only to 4.77% at 70 °C. The samples also retain water after desorption at these temperatures: 0.98 at 55 °C and 0.22 °C. It is assumed that hydrogen bonds are established between sample and water molecules retaining them even after desorption. If the amount of water retained in the sample increases when temperature rises from room temperature to 55 °C, by further increasing temperature to 70 °C, this decreases, probably due to the thermal destruction of these links. Similarly, the maximum sorption capacity decreased when the temperature rose above 55 °C. The fact that there is no mass loss certifies that the compound does not decompose in wet atmosphere at room temperature.

The packing model developed on the basis of X-ray crystallographic data (Fig. 3) reveals the existence of the voids within the supramolecular structure in which different guests molecules might be accommodated in amounts depending on their size. The *gas storage capacity* might be theoretical estimated by the accessible void volume for the guest molecules, either on the basis of the solvent accessible surface (mapped out by the centre of probe spheres) or contact surface (mapped out by the probe's surface). These are 3D visualized and quantitative mapped by Mercury software package on the basis of the crystallographic data. For this purpose the atomic radius value of the molecule sample is entered in software which automatically calculates the theoretical value of the occupied volume. The calculated data for a series of gases as probes are presented in Table 4. From the results presented in Table 4 it can see that as expected, small hydrogen and helium molecules are accessible in the highest amounts.

In order to study the stability of compound **1** in solution (2 mg in 1 mL methanol), ATR-FTIR technique was used. The solution containing copper complex was applied on the ZnSe crystal surface and the spectra were registered every minute until the solvent evaporated, by using repeating measurements experiment at room temperature, the spectra being presented in Fig. 4.

At the first registration, in the FTIR spectra are mainly present the specific absorption bands of methanol which is in high amount in the mixture: broad band around 3400 cm^{-1} (OH groups) as well as the narrow bands at 2945 and 2883 cm^{-1} (—CH_3 groups) and 1660 cm^{-1} (ν_{OH} group). As the methanol evaporates, the spectrum of the compound is increasingly better contoured with its characteristic bands (Fig. 4b). During solvent evaporation, the hydrogen bonds between coordinated water molecules, imidazole and carboxylic acid were reformed and all the characteristic bands of the compound **1** appear at about the same wave number as in the spectrum registered in solid state: 3348 and 3096 cm^{-1} (ν_{OH} for free and H-bond groups), 1651 cm^{-1} (carboxylate C=O), 1574 cm^{-1} (C=N from pyridine ring), 1269 cm^{-1} (Si—CH_3), 1030 cm^{-1} (Si—O—Si) indicating the regeneration of the initial structure. The broad bands in the range 2400–2700 cm^{-1} are attributed to the hydrogen bonds. The deconvoluted IR spectra in the 2400–3800 cm^{-1} region (Fig. 4S) better emphasize the compound reformation as the solvent was evaporated.

The dynamic of the hydrogen bonds with temperature in the compound **1** has been studied by using a FTIR-ATR spectrometer equipped with a temperature controller. The spectra (Fig. 5S) were recorded at each increase in temperature by 5 °C up to the first thermal decomposition stage (140 °C) as evidenced by thermogravimetrical analysis (Fig. 2S and Table 3). The thermally induced structural changes can be seen in the Fig. 5S. During the heating, specific broad bands of the OH stretching vibrations at 3720 cm^{-1} appear in the spectra of compound **1** due to breaking hydrogen bonds present in the region 3300–3120 cm^{-1}. By cooling with the same rate, the initial spectrum is obtained, indicating reformation of the hydrogen bonds between carboxylic OH groups and imidazole.

Table 4
The theoretically estimated void volume values of the crystalline compound accessible for different gases.

Gas	Radius (Å)	Contact surface area		Solvent accessible surface	
		x % of unit cell volume	Void volume (Å^3)	x % of unit cell volume	Void volume (Å^3)
Hydrogen	0.37	11.1	282.47	9.6	244.43
Helium	0.32	13.6	345.06	12.4	314.60
Oxygen	0.73	4.5	114.11	1.0	25.57
Nitrogen	0.75	3.9	3.9	0.8	21.20
Chlorine	0.99	0.5	11.85	–	0.62
Carbon monoxide	1.128	–	–	–	–

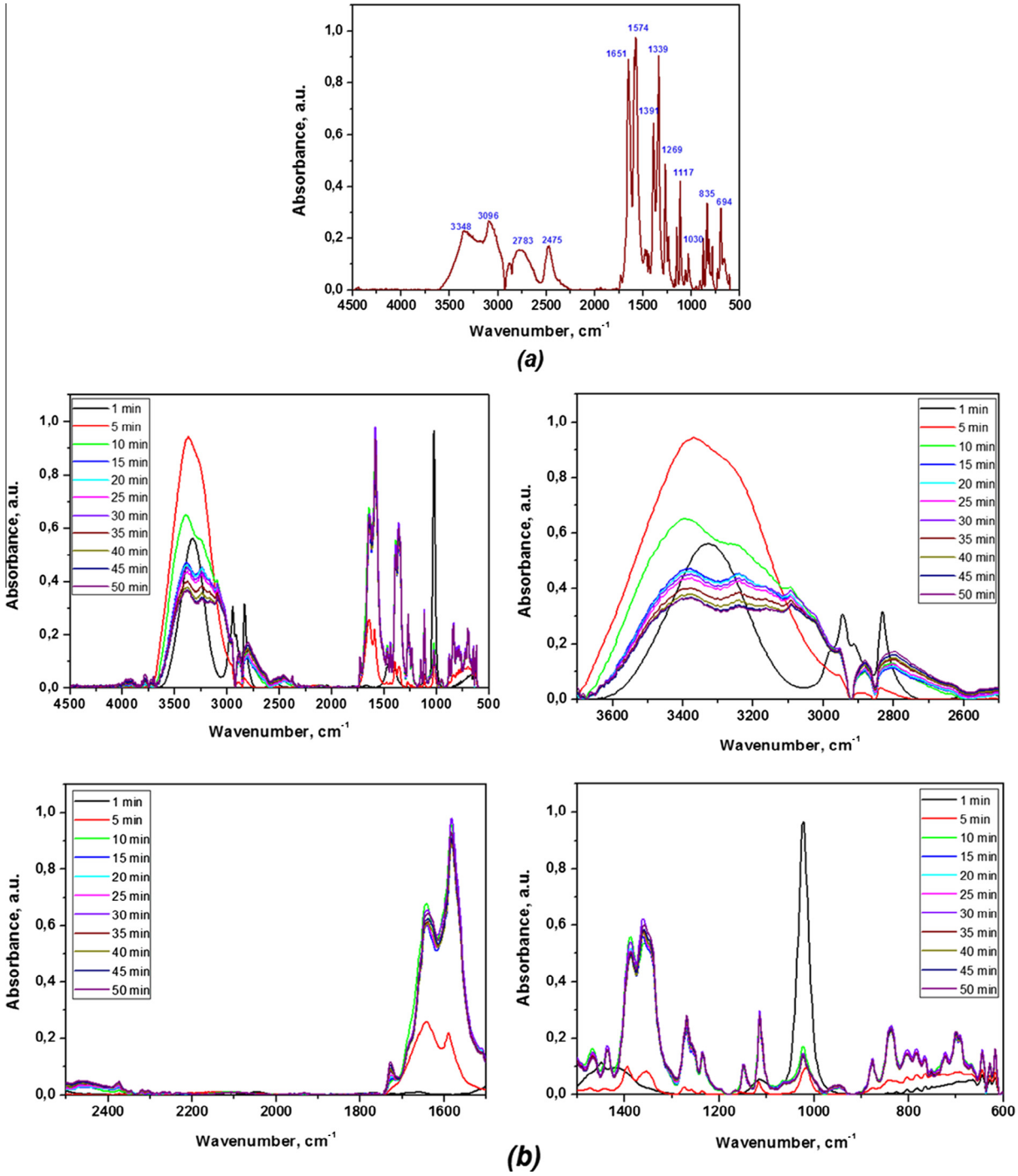

Fig. 4. ATR-FTIR spectra of compound **1** before dissolving in methanol (***a***) and during the evaporation of methanol (***b***).

Conclusion

By sequential treating of 2,3-pyridinedicarboxylic anhydride with 1,3-bis(3-aminopropyl)tetramethyldisiloxane and $CuCl_2$, the copper complex of the proper dicarboxylic acid resulted while the diamine complexed with chlorine anion forming chlorohydrate. The two entities self-assembled through N—H···O and N—H···Cl hydrogen-bonding interactions forming a 3D supramolecular architecture elucidated by single crystal X-ray diffraction and spectral analysis. This assembly is preserved by dissolution in polar solvent and subsequently solvent evaporation as well as by heating up to 140 °C as was highlighted by the ATR-FTIR. Over this temperature the thermal degradation of the product starts with loss of mass, as thermogravimetric analysis results showed. The supramolecular structure showed low porosity able to host in reasonable amounts only small molecules such as hydrogen and helium as was theoretical estimated. The structure reported in this article could be considered as a sensitive one that changes reversibly under the action of a stimulus, such as solvent traces or temperature. By the modification within structure, the strength of the intermolecular interactions could be varied and this it will be our aim in a future work.

Acknowledgements

This work was supported by a grant of the Ministry of National Education, CNCS – UEFISCDI, Program PN-II-Capacities, Modul III, Romania – Moldova Bilateral Cooperation (Project ComSilBio, Contract 690/16.04.2013).

Appendix A. Supplementary material

Supplementary data associated with this article can be found, in the online version, at http://dx.doi.org/10.1016/j.molstruc.2014.11.038.

References

[1] X.-Z. Liu, L.-M. Fan, Z. Sun, W. Zhang, Y.-S. Ding, X.-T. Zhang, Chin. J. Struct. Chem. 32 (7) (2013) 1062–1066.
[2] S. Chauhan Jayprakash, V. Pandya Ajit, Int. J. Eng. Sci. Inv. 2 (2013) 36–43. and references herein.
[3] N. Vachirapatama, N. Theerapittayatakul, J. Sci. Technol. 34 (3) (2012) 303–307.
[4] E. Norkus, E. Gaidamauskas, I. Stalnioniene, D.C. Crans, Heteroatom Chem. 16 (4) (2005) 285–291.
[5] M.P. Brandi-Blanco, D. Choquesillo-Lazarte, C.G. Garcia-Collado, J.M. Gonzalez-Perez, A. Castineiras, J. Niclos-Gutierrez, Inorg. Chem. Comm. 8 (2005) 231–234.
[6] C.-M. Liu, D.-Q. Zhang, D.-B. Zhu, Inorg. Chem. Commun. 11 (2008) 903–906.
[7] E. Soleimani, J. Mol. Struct. 995 (2011) 1–8.
[8] H. Yin, S.-X. Liu, J. Mol. Struct. 918 (2009) 165–173. and references herein.
[9] H. Yin, S.X. Liu, J. Mol. Struct. 29 (2009) 165–173.
[10] L.I. Wei, L.I. Chang-Hong, L.I. Heng-Feng, X.U. Jin-Sheng, L.I. Li, Chin. J. Struct. Chem. 32 (10) (2013) 1567–1571.
[11] B.O. Patrick, C.L. Stevens, A. Storr, R.C. Thompson, Polyhedron 22 (2003) 3025.
[12] S. Yan, X. Li, X. Zheng, J. Mole. Struct. 929 (2009) 105–111.
[13] Y.A. Ammar, Y.A. Mohamed, A.M.Sh. El-Sharief, M.S.A. El-Gaby, S.Y. Abbas, Reactivity of 2, J. Chem. Sci. CSJ 16 (2011) 1–11.
[14] M. Simionescu, M. Marcu, M. Cazacu, Eur. Polym. J. 39 (2003) 777–784.
[15] M. Cazacu, A. Vlad, M. Marcu, C. Racles, A. Airinei, G. Munteanu, Macromolecules 39 (2006) 3786–3793.
[16] E. Hamciuc, C. Hamciuc, M. Cazacu, M. Ignat, G. Zarnescu, Eur. Polym. J. 45 (1) (2009) 182–190. ISSN 0014-3057.
[17] E. Hamciuc, C. Hamciuc, M. Cazacu, Eur. Polym. J. 43 (2007) 4739–4749.
[18] M. Cazacu, A. Vlad, A. Airinei, A. Nicolescu, I. Stoica, Dyes Pigm. 90 (2011) 106–113.
[19] M. Alexandru, M. Cazacu, A. Arvinte, S. Shova, C. Turta, B.C. Simionescu, A. Dobrov, E.C.B.A. Alegria, Eur. J. Inorg. Chem. (2014) 120–131.
[20] A. Soroceanu, M. Cazacu, A. Nistor, S. Shova, Rev. Roum. Chim. 58 (2–3) (2013) 209–216.
[21] M.-F. Zaltariov, M. Cazacu, N. Vornicu, S. Shova, C. Racles, M. Balan, C. Turta, Supramol. Chem. 25 (8) (2013) 490–502.
[22] A. Soroceanu, M. Cazacu, S. Shova, C. Turta, J. Kožišek, M. Gall, M. Breza, P. Rapta, T.C.O. Mac Leod, A.J.L. Pombeiro, J. Telser, A.A. Dobrov, V.B. Arion, Eur. J. Inorg. Chem. (2013) 1458–1474.
[23] A. Vlad, C. Turta, M. Cazacu, E. Rusu, S. Shova, Eur. J. Inorg. Chem. 31 (2012) 5078–5084.
[24] M. Cazacu, A. Vlad, G. Munteanu, A. Airinei, J. Polym. Sci., Part A: Polym. Chem. 46 (5) (2008) 1862–1872.
[25] A. Vlad, M. Cazacu, G. Munteanu, A. Airinei, P. Budrugeac, Eur. Polym. J. 44 (2008) 2668–2677.
[26] P. Mukherjee, C. Biswas, M.G.B. Drew, A. Ghosh, Polyhedron 26 (2007) 3121–3128.
[27] CrysAlis RED, Oxford Diffraction Ltd., Version 1.171.36.32, 2003.
[28] O.V. Dolomanov, L.J. Bourhis, R.J. Gildea, J.A.K. Howard, H. Puschmann, J. Appl. Cryst. 42 (2009) 339–341.
[29] G.M. Sheldrick, Acta Crystallogr. A64 (2008) 112–122.